Influence of Ni on the thermoelectric properties of the partially filled calcium skutterudites CayCo4 – xNi xSb12

M. Puyet, A. Dauscher, Bertrand Lenoir, C. Bellouard, C. Stiewe, Etienne Muller, J. Hejtmanek, J. Tobola

Influence of Ni on the thermoelectric properties of the partially filled calcium skutterudites $Ca_yCo_{4-x}Ni_xSb_{12}$

M. Puyet, A. Dauscher, and B. Lenoir*
Laboratoire de Physique des Matériaux, Nancy-Université, CNRS, Ecole Nationale Superieure des Mines de Nancy, Parc de Saurupt, F-54042 Nancy, France

C. Bellouard
Laboratoire de Physique des Matériaux, Nancy-Université, CNRS, BP 239, 54506 Vandoeuvre les Nancy Cedex, France

C. Stiewe and E. Müller
German Aerospace Center (DLR), Institute of Materials Research, Linder Hoehe, 51147 Cologne, Germany

J. Hejtmanek
Institute of Physics, Academy of Sciences of the Czech Republic, Cukrovarnicka 10, CZ-162 53 Praha 6, Czech Republic

J. Tobola
Faculty of Physics and Applied Computer Science, AGH University of Science and Technology, 30-059 Krakow, Poland
(Received 22 December 2006; revised manuscript received 3 April 2007; published 13 June 2007)

We have synthesized and studied the structural and thermoelectric properties of Ni-substituted partially filled $Ca_yCo_{4-x}Ni_xSb_{12}$ ($y\sim0.10$ and 0.18; $0<x<0.10$) skutterudites. Electrical and thermal properties have been measured in a wide range of temperature (2–800 K). It was found that the presence of Ni increases drastically the dimensionless figure of merit at moderated temperature with respect to the Ni-free analogous samples. These greater thermoelectric properties are discussed in view of electronic structure features near E_F as resulted from KKR-CPA calculations. Both experimental findings and computed DOS characteristics point to the conclusion that another channel of electrical conductivity, related to the presence of *d*-Ni states and opening additional electron Fermi surface pocket, is presumably responsible for the drop of electrical resistivity with respect to the Ni-free samples. In the same time, important DOS variations near E_F were found in $Ca_yCo_{4-x}Ni_xSb_{12}$, as previously in $Ca_yCo_4Sb_{12}$. This gives rise to a large thermopower detected in the two series of compounds.

DOI: 10.1103/PhysRevB.75.245110 PACS number(s): 71.20.Nr, 72.20.Pa, 75.20.Ck

I. INTRODUCTION

Some of the semiconductors that have been recently proposed as possible thermoelectric materials have complex open crystal structures with many atoms per unit cell.[1] Among them, the skutterudite family of materials namely based on $CoSb_3$ shows great promise with thermoelectric performance exceeding those of state-of-the-art thermoelectric materials.[1–3] Actually, the dimensionless figure of merit $ZT=S^2T/\rho\lambda$, where S is the thermoelectric power, ρ the electrical resistivity, λ the thermal conductivity ($\lambda=\lambda_l+\lambda_e$, where λ_l is the lattice thermal conductivity and λ_e the electronic thermal conductivity) and T the absolute temperature, was found to exceed unity at moderated temperature.

N-type electrical conductivity can be achieved in partially filled skutterudites of general formula $R_yCo_4Sb_{12}$ with R, the filler atom, such as Ca, Sr, Ba, Tl, Sn, In, Ge, Ce, La, Eu, Nd, Yb.[4–16] The case of alkaline earths proved to be particularly interesting as the limit filling fraction y_m in these materials is greater than 0.10 and increases when passing from Ca[17] ($y_m=0.20$) to Ba[10] ($y_m=0.44$). A high limit filling fraction is undoubtedly an asset to vary simultaneously the electron carrier concentration and decrease the thermal conductivity. It is expected that the higher the filling fraction is, the more the thermoelectric properties can be tuned. This is effectively observed experimentally: the thermoelectric properties are improved when passing from Ca to Ba.[10,14]

The high electrical resistivity obtained in the $Ca_yCo_4Sb_{12}$ skutterudites[14] is one of the factors that limits the achievement of attractive thermoelectric performance. An efficient modulation of the electrical properties can be expected through the modification of the carrier concentration in the material. Many ways can be considered to achieve this goal. First of all, one can imagine to fill the cavities with higher calcium contents than the current solubility limit ($y_m=0.20$) thanks to an adapted substitution of either the cobalt or the antimony atoms to compensate the excess of electrons induced by the presence of greater amounts of Ca. This approach was successfully used by Lamberton *et al.*[11] for the $Eu_yCo_4Sb_{12-x}Ge_x$ compounds: the charge compensation gave rise to an improvement of the thermoelectric performance. However, other studies showed that this is not the most efficient way to improve the thermoelectric properties. For instance, Dilley *et al.*[6] showed that by substituting Sb by Sn atoms in $Yb_yCo_4Sb_{12-x}Sn_x$ skutterudite compounds, the charge compensation in the *n*-type samples resulted in a decrease of the *ZT* values. Other works on partially filled skutterudites led to similar conclusions.[18]

Another attempt to lower the electrical resistivity, without substantial decrease of the thermopower, consists in the

n-type "doping" of the material by substituting Co or Sb atoms by elements with more valence electrons. Several research groups controlled the electron carrier concentration in the binary $CoSb_3$ skutterudite by partial substitutions of Ni, Pt, or Pd on the Co sites or Te on the Sb sites.[19–26] Among all these works, the alloying with nickel deserves a special attention. It was reported that the presence of a minute amount of Ni in $CoSb_3$ results in a substantial decrease of the electrical resistivity and at the same time to a decrease of the total thermal conductivity, leading to particularly attractive thermoelectric properties.[19,22] In the first investigations of Dudkin and Abrikosov,[19] it was concluded that the presence of less than 1 at. % of Ni does correct the defects and the inherent distortions of the crystallographic skutterudite structure, resulting in an increase of both the microhardness and the mobility of the charge carriers.

In further studies, Dyck *et al.*[27] showed that nickel has also a very positive influence on the thermoelectric properties of *n*-type Co_4Sb_{12} skutterudites partially filled with barium. A dimensionless figure of merit *ZT* as high as 1.2 at 800 K was achieved for the $Ba_{0.3}Co_{3.95}Ni_{0.05}Sb_{12}$ composition. Similar trends have been underlined in Ca- and Sr-partially filled skutterudites.[28,29] Thus, nickel alloying seems to be an effective mean to optimize the thermoelectric properties of skutterudite materials based on $CoSb_3$.

In this paper, we report on the study of the influence of nickel on the electrical and thermal properties of two series of $Ca_yCo_{4-x}Ni_xSb_{12}$ samples: first one with $y \sim 0.10$ and the second one with $y \sim 0.18$. The transport properties were measured between 2 and 800 K, and in parallel, electronic structure calculations have been performed to better understand the role of Ni in these materials.

II. EXPERIMENTAL AND COMPUTATIONAL DETAILS

The two series of $Ca_yCo_{4-x}Ni_xSb_{12}$ samples have been prepared by a solid-state reaction method. Appropriate quantities of high purity Ca pellets (99.5%), Sb shots (99.999%), Co (99.998%), and Ni (99.995%) powders were loaded into a quartz ampoule. The ampoule was sealed under a reducing $He-H_2$ atmosphere and heated in a vertical oscillating furnace up to 1023 K for 84 h with the heating rate fixed at 1 K min^{-1}. The grown ingot was then ground in an agate mortar into powders ($\sim$100 μm) that were annealed under the same previous conditions. The resulting ingot was again powdered and the powders were pressed into pellets that were annealed at 893 K for 84 h. These pellets were crushed and powdered ($<$50 μm). Final compaction was performed in graphite dies by hot pressing in an argon atmosphere at 873 K for 2 h under 51 MPa. The resulting Ni-containing ingots of 15 mm in diameter exhibit densities higher than 93% of the theoretical densities.

X-ray diffraction (XRD) and electron microprobe analyses (EPMA) data show that a homogeneous skutterudite phase is obtained in all prepared samples together with two minor secondary phases: pure Sb and a Ca-rich phase. These two impurity phases were also present in the Ni-free samples.[17] Typical XRD pattern of a $Ca_yCo_{4-x}Ni_xSb_{12}$ sample is shown in Fig. 1. In Table I are listed the actual

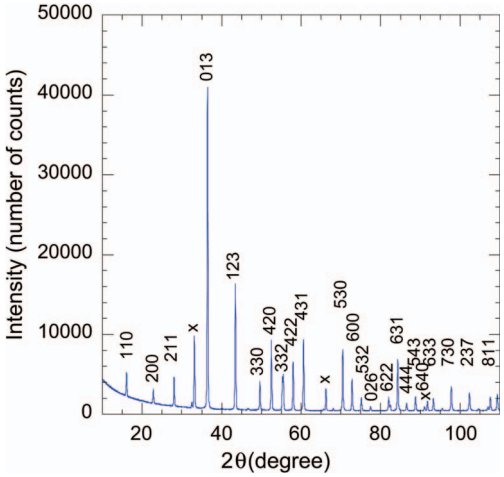

FIG. 1. (Color online) Illustrative X-ray diffraction pattern obtained for the $Ca_yCo_{4-x}Ni_xSb_{12}$ skutterudites. All the peaks have been indexed with regard to the JCPDS file pattern *n*°78–976. x corresponds to Si peaks (Si powder has been added to normalize the angular position of the $Ca_yCo_{4-x}Ni_xSb_{12}$ peaks).

chemical compositions of the two series of skutterudites prepared, as determined from EPMA.

For the transport studies, bar, disk, or square shaped specimens were cut with a diamond wire saw in the densified materials. Low temperature transport properties (electrical resistivity, thermopower and thermal conductivity) were measured from 10 to 300 K by a longitudinal steady-state method in an automated closed-cycle refrigerator system. Fine chromel-constantan thermocouples were used. Magnetotransport measurements, including magneto-resistance and Hall measurements, were performed with an AC transport measurement system option of the PPMS (Quantum Design) over the temperature range 2–300 K and under a magnetic field ranging up to 7 T. Ohmic contacts to the samples were made with fine copper wires attached with care using a tiny amount of silver paint. For the high temperature measurements covering the range 300–800 K, other techniques have been employed. The thermopower was measured by a standard method using a home-made apparatus.[30] The electrical resistivity was determined by a four probe technique based on the Van der Pauw method. The thermal conductivity was evaluated by measuring both the thermal diffusivity using a home-made laser flash apparatus and the density calculated from mass and volume measurements at ambient temperature. No correction for thermal expansion at high temperature was made.

A good agreement was observed at room temperature between the low and high temperature transport measurements. The deviation does not exceed 12%.

In order to elucidate the electron transport properties of Ca-filled skutterudites alloyed with Ni, electronic structure calculations have been performed on $Ca_yCo_{4-x}Ni_xSb_{12}$ skutterudites for $y=0.1$ and 0.2 and for $x=0$, 0.01, 0.04, and 0.08 using the Korringa-Kohn-Rostoker method combined with the coherent potential approximation (KKR-CPA).[31] Disorder effects have been treated parallel on two crystallographic sites (Co/Ni and vacancy/Ca). The crystal potential of

TABLE I. Some properties of $Ca_yCo_{4-x}Ni_xSb_{12}$ skutterudites. All the compositions given have been normalized to full occupancy of the cobalt site and correspond to the actual composition. a is the lattice parameter. The reported values of Hall carrier concentration, n, and Hall mobility, μ_H, are for room temperature measurements. The value of the exponent, p, ($\mu_H \sim T^p$ for $T > 100$ K) is also given.

Sample $n°$	Compound	a Å	n cm^{-3}	μ_H $cm^2/V\,s$	p
1	$Ca_{0.08}Co_4Sb_{12.45}$	9.0423	3.2×10^{20}	5.5	−1.7
2	$Ca_{0.08}Co_{3.98}Ni_{0.02}Sb_{12.15}$	9.0423	1.3×10^{20}	28.6	−0.6
3	$Ca_{0.10}Co_{3.98}Ni_{0.02}Sb_{12.15}$	9.0436	1.6×10^{20}	29.7	−0.9
4	$Ca_{0.10}Co_{3.95}Ni_{0.05}Sb_{12.34}$	9.0437	2.4×10^{20}	20.9	−0.6
5	$Ca_{0.20}Co_4Sb_{12.46}$	9.0498	2.8×10^{20}	7.3	−1.3
6	$Ca_{0.15}Co_{3.98}Ni_{0.02}Sb_{11.80}$	9.0484	3.1×10^{20}	20.1	−0.9
7	$Ca_{0.18}Co_{3.97}Ni_{0.03}Sb_{12.40}$	9.0488	4.4×10^{20}	24.5	−0.7
8	$Ca_{0.18}Co_{3.94}Ni_{0.06}Sb_{12.40}$	9.0489	5.3×10^{20}	19.0	−0.8

muffin-tin form has been constructed within the local density approximation (LDA) framework, employing von Barth-Hedin formula for the exchange-correlation part. For fully converged potentials, total and site decomposed as well as l-decomposed density of states (DOS) were calculated using the tetrahedron method for integration in the reciprocal space. Furthermore, the generalized Lloyd formula[32] was used to allow for precise determination of the Fermi level (without making integration over occupied electronic states). The experimental values of lattice parameters determined from XRD (Table I) were employed in this study. More details concerning the KKR-CPA methodology can be found in Refs. 31–33.

As it was particularly difficult to reproduce exactly the same calcium content in each of the two series of skutterudites prepared (see Table I), the exact role of Ni substitution will be essentially qualitatively understood within each series.

III. RESULTS AND DISCUSSION

A. Transport and magnetotransport properties

The temperature dependences of the electrical resistivity measured for the two series of considered samples are shown in Fig. 2. The presence of Ni strongly decreases the value of the electrical resistivity between 20 and 500 K for the first series of samples [$y \sim 0.10$, Fig. 2(a)]. The decrease is still more spectacular for the second series [$y \sim 0.18$, Fig. 2(b)]. The obtained values at room temperature are in the range 6.10^{-4} to 15.10^{-4} Ω cm for the Ni-containing samples. These values are typically those encountered in Ni-free partially filled n-type skutterudites for filler atom contents similar to those of this study.[8,10] We can also note that for temperatures higher than 30 K, all the Ni-containing compounds possess a positive temperature coefficient of resistivity. This behavior is typical of that of a degenerate semiconductor.

As expected, the Hall coefficient, R_H, of the Ni-containing samples is negative in the whole temperature range investigated (Fig. 3). Moreover, their temperature dependences are less pronounced than the dependences observed for the Ni-free samples. Since nickel possesses one more electron than cobalt, one would expect an increase of the carrier concentration in the presence of Ni. It means, considering a model with only one type of carrier, that the absolute value of R_H

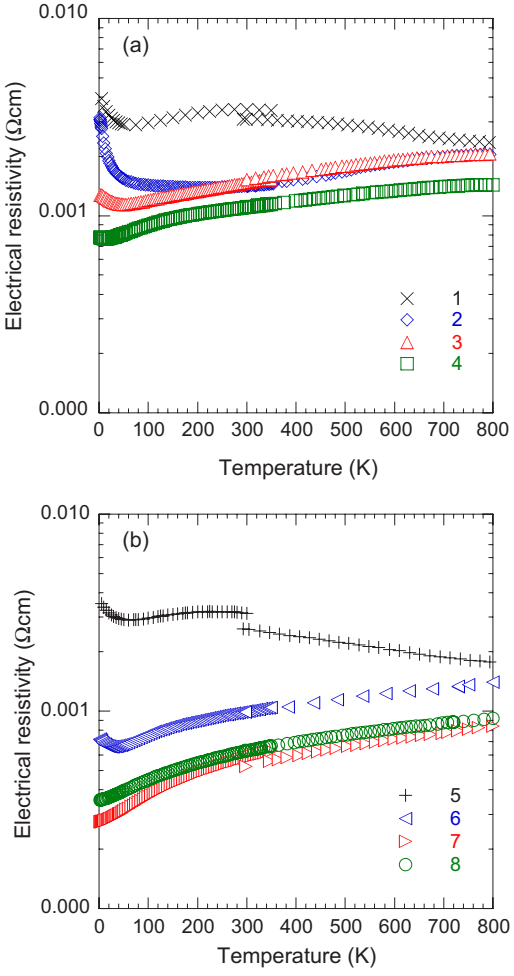

FIG. 2. (Color online) Temperature dependences of the electrical resistivity ρ for the two series of $Ca_yCo_{4-x}Ni_xSb_{12}$ skutterudites. (a) $y \sim 0.10$; (b) $y \sim 0.18$. The symbols refer to the sample numbers given in Table I for the different compounds studied.

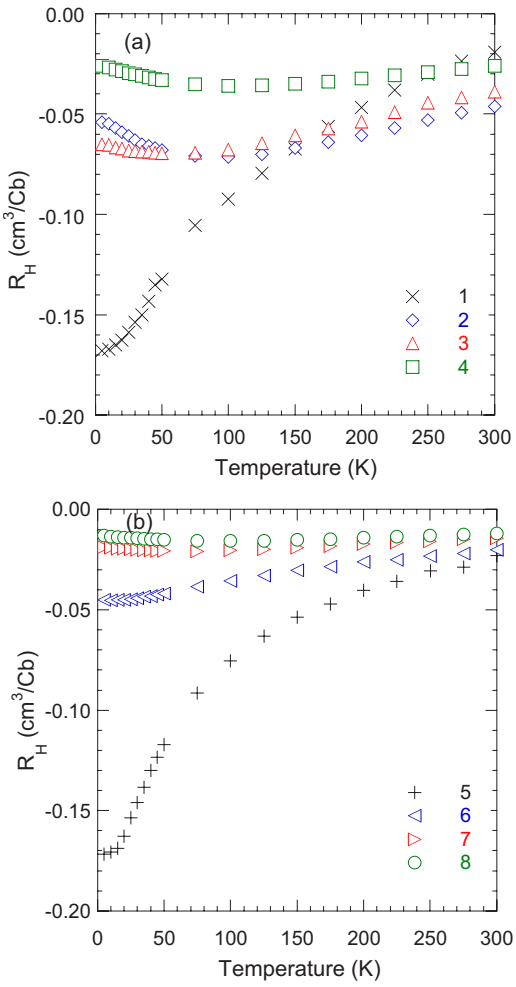

FIG. 3. (Color online) Temperature dependences of the Hall coefficient R_H for the two series of $Ca_yCo_{4-x}Ni_xSb_{12}$ skutterudites. (a) $y \sim 0.10$; (b) $y \sim 0.18$. The symbols refer to the sample numbers given in Table I for the different compounds studied.

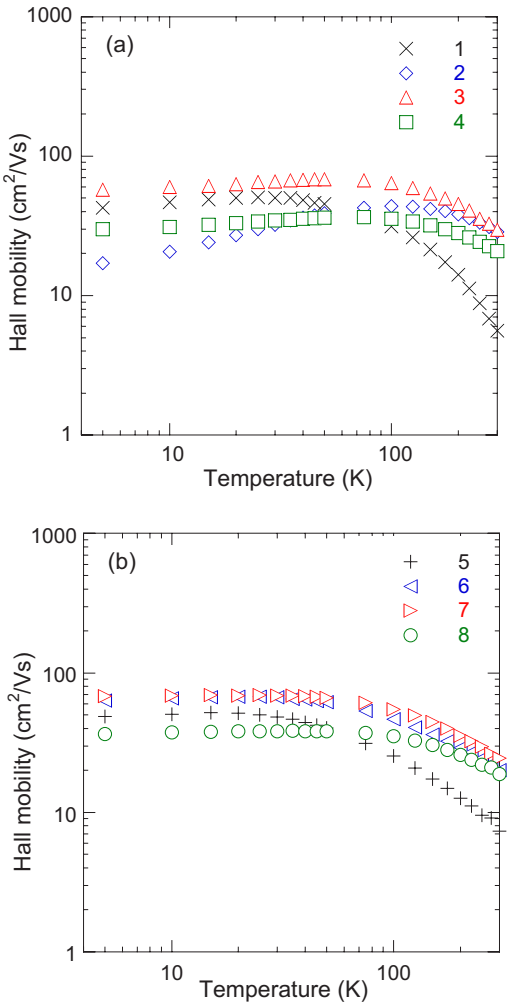

FIG. 4. (Color online) Temperature dependences of the Hall mobility μ_H for the two series of $Ca_yCo_{4-x}Ni_xSb_{12}$ skutterudites. (a) $y \sim 0.10$; (b) $y \sim 0.18$. The symbols refer to the sample numbers given in Table I for the different compounds studied.

will be weaker. These anticipations are quite well respected in the series $y \sim 0.18$ between $0 < T < 300$ K [Fig. 3(b)] while the tendency is less clear for the series $y \sim 0.10$ [Fig. 3(a)]. The values of the Hall carrier concentrations, n, at room temperature extracted from the simple relation $R_H = 1/ne$ (with e the elementary charge) are reported in Table I.

The temperature dependences of the Hall mobility, μ_H, for the two families of compounds are given in Fig. 4. For $T < 100$ K, no general tendency can be put forward on the behavior of μ_H when cobalt atoms are substituted by nickel atoms. The mobility slowly increases with temperature for the series where $y \sim 0.10$. The modifications with temperature are even less pronounced for the series with $y \sim 0.18$. For $T > 100$ K, the mobility of the alloyed samples exceeds systematically the mobility of the Ni-free samples. The values achieved at room temperature are about five and three times greater in the alloyed samples, for y contents of 0.10 and 0.18, respectively (Table I). Moreover, for $T > 100$ K, in the presence of nickel, the μ_H temperature dependence behavior can be fitted by a power law of the form T^p with $-0.9 \leqslant p \leqslant -0.6$ (Table I). For the Ni-free samples, p is close to -1.5.[34] It should be underlined that a similar change of slope in the μ_H behavior has also been observed in $Ba_yCo_{4-x}Ni_xSb_3$ by Dick *et al.*,[27] but their values were found to decrease with increasing the Ni content near room temperature. These authors explained that the change of slope of the Hall mobility near room temperature is related to a change in the scattering mechanisms by invoking that the scattering by the acoustic phonons ($p = -1.5$) is no more the main scattering mechanism and that an additional scattering mechanism must be involved in the Ni-containing samples. Since nickel acts as an electron donor, they attributed the additional mechanism to the presence of ionized Ni impurities. In view of the analysis of the electronic structure in the $Ca_yCo_{4-x}Ni_xSb_{12}$ compounds (see Sec. III C), the change of slope of μ_H versus T near room temperature in the Ni containing samples should be rather linked to a mixed conduction phenomena with the presence of "light" electrons responsible for the increase of the mobility.

The influence of nickel substitution on the thermoelectric power is presented in Fig. 5. The thermoelectric power of the alloyed samples always exhibits an almost linear temperature dependence between 0 and 300 K, behavior that is consistent

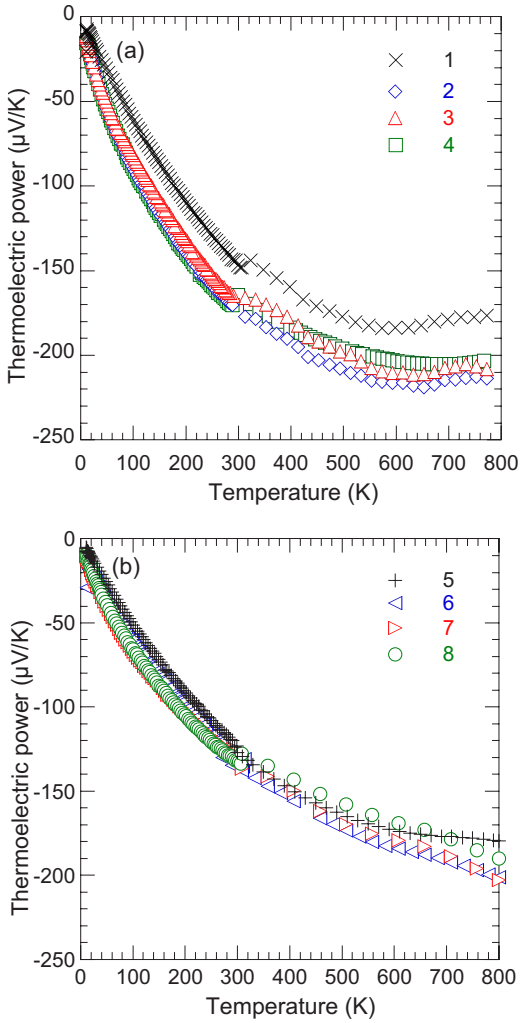

FIG. 5. (Color online) Temperature dependences of the thermoelectric power S for the two series of $Ca_yCo_{4-x}Ni_xSb_{12}$ skutterudites. (a) $y \sim 0.10$; (b) $y \sim 0.18$. The symbols refer to the sample numbers given in Table I for the different compounds studied.

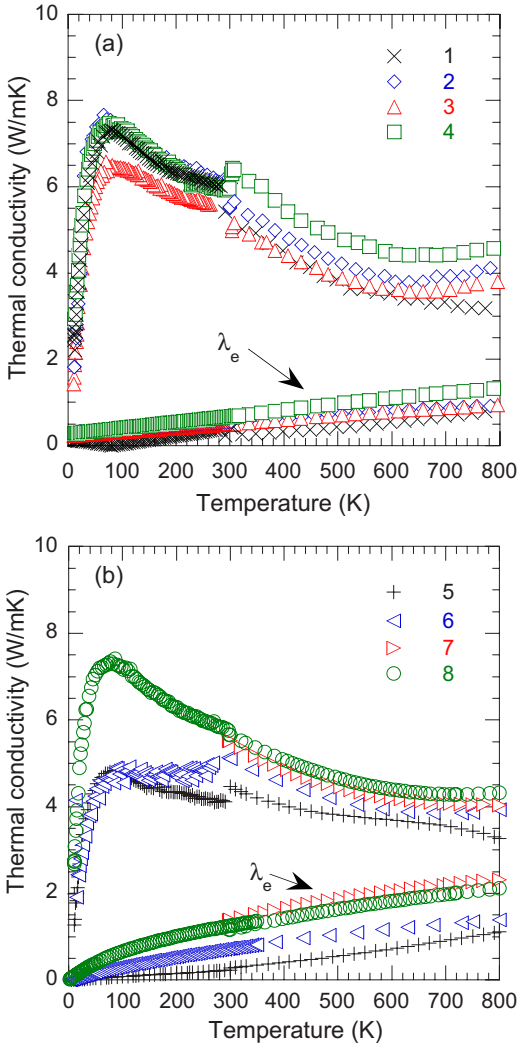

FIG. 6. (Color online) Temperature dependences of the total thermal conductivity λ and of the electronic thermal conductivity (λ_e) for the two series of $Ca_yCo_{4-x}Ni_xSb_{12}$ skutterudites. (a) $y \sim 0.10$; (b) $y \sim 0.18$. The symbols refer to the sample numbers given in Table I for the different compounds studied.

with that of a degenerate electron gas. At higher temperature, the holes also contribute to conduction, leading to a decrease of the absolute value of the thermoelectric power for the series of compounds with $y \sim 0.10$. The influence of the minority carriers is not perceptible for the second series of compounds ($y \sim 0.18$), due to a higher electron concentration. Thus the thermoelectric power continues to increase between 300 and 800 K. Intriguing is the fact that although the density of carriers increases in the presence of nickel, the absolute values of the thermoelectric power do not weaken drastically for the two series of samples. Similar observations were reported earlier by Dyck *et al.*[27] for Ba-partially filled skutterudites alloyed with nickel.

The thermal properties of the different samples are represented between 4 and 800 K in Fig. 6. The temperature dependences behaviors of the Ni-free and Ni-containing samples are similar. It is difficult to analyze the true influence of nickel from these dependences because the thermal properties are highly dependent on the alkaline earth content,[35] and as already mentioned, we were not able to reproduce exactly the same calcium content from one sample to another. Anyway, the substitution of nickel on the cobalt sites should not fundamentally modify phonons-point defects scattering mechanisms because the weight and the size of Co and Ni are very close. It is however possible that electron-phonon scattering mechanisms appear considering the increase of the carrier density. At room temperature, the thermal conductivity of the Ni-free skutterudites is mainly due to the lattice thermal conductivity.[35] This is no more completely true in the Ni-containing samples for which the electronic thermal conductivity increases after the significant reduction of the electrical resistivity. The electronic contributions to the total thermal conductivity are visualized on Fig. 6 for both series of samples. They have been calculated assuming the validity of the Wiedeman-Franz law, $\lambda_e = L_0 T/\rho$ with $L_0 = 2.45 \times 10^{-8}$ W Ω K^{-2}.

The temperature dependences of the dimensionless figure of merit ZT are reported in Fig. 7 for the two series of Ni-containing skutterudites, in the 300–800 K temperature

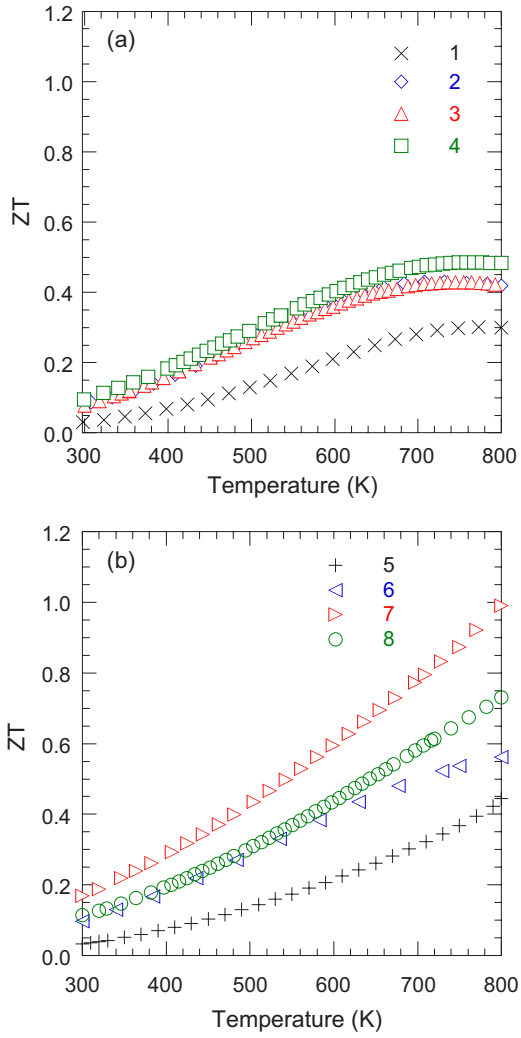

FIG. 7. (Color online) Temperature dependences of the dimensionless figure of merit ZT the two series of $Ca_yCo_{4-x}Ni_xSb_{12}$ skutterudites. (a) $y \sim 0.10$; (b) $y \sim 0.18$. The symbols refer to the sample numbers given in Table I for the different compounds studied.

range where the thermoelectric performance are the most interesting. The introduction of nickel in the $Ca_yCo_4Sb_{12}$ structures results in an increase of the dimensionless figure of merit in the whole temperature range. One notes an increase of the order of 40–65 % of the ZT value at $T=800$ K in the series $y \sim 0.10$. The enhancement is even more spectacular in the second series and reaches more than 100% at $T=800$ K. To the best of our knowledge, we are not aware of such a huge effect due to alloying on the thermoelectric properties of a material.

The partial filling of the constitutional voids of the Co_4Sb_{12} skutterudite by calcium atoms, coupled with nickel alloying, allows reaching a ZT value close to unity at 800 K for the $Ca_{0.18}Co_{3.97}Ni_{0.03}Sb_{12}$ compound. It is one of the best n-type compounds of the skutterudites family produced until now.

B. Electronic structure calculations

According to numerous electronic structure calculations in pure $CoSb_3$, the deep valley of density of states between

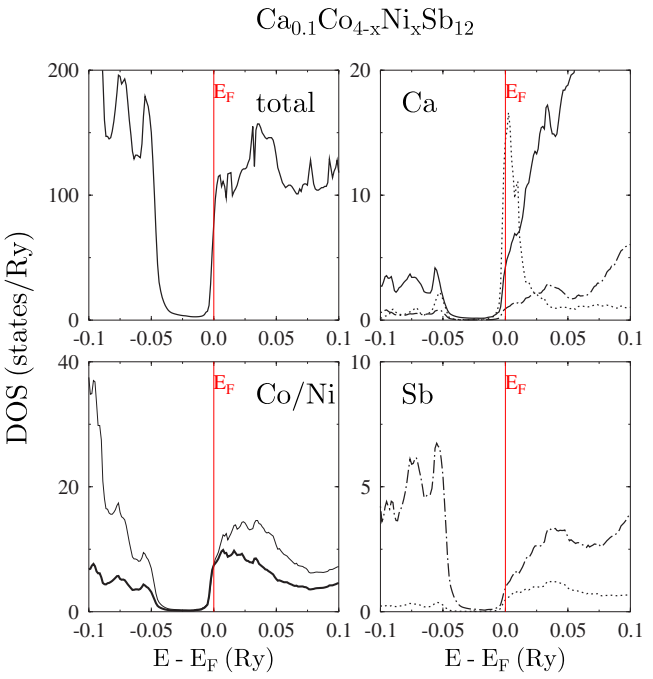

FIG. 8. (Color online) KKR-CPA density of states in $Ca_{0.10}Co_{4-x}Ni_xSb_{12}$ ($x=0.04$). Total and l-decomposed DOS (s—dotted, p—dot-dashed, d—full lines) of constituent atoms are shown. In the case of Co (thin line) and Ni (thick line), s and p contributions are not plotted for sake of clarity. $E_F=0$ is marked by a vertical red line.

the valence and conduction bands (of the order of 0.5 eV) arises from strong hybridization of d-Co states and p-Sb states.[25,34,36–40] The presence of this deep valley can also be detected on the total DOS, $N_{tot}(E_F)$, calculated for disordered $Ca_yCo_{4-x}Ni_xSb_{12}$ skutterudites from the KKR-CPA method (Figs. 8 and 9). The computed dispersion curves $E(k)$ in $CoSb_3$ showed either very low DOS (with a quasilinear band crossing the valley[36]) or a true energy gap at the Fermi level.[25,34,36–40] It was also found that the calculated ground state properties of $CoSb_3$ are sensitive to the choice of the crystal structure parameters, and particularly to the positional parameters of the antimony atoms (scale of the metalloid rings size, characteristics of the skutterudite structure).[25,37] Slightly different interatomic distances used in different calculations presumably lead to different overlapping of the wave functions between Sb and Co and to different values of the energy gap (ranging from 0.1 to 0.5 eV).

Our previous study on partially filled $Ca_yCo_4Sb_{12}$ skutterudites showed that calcium inserted into the cavity behaves as an electron donor resulting from the presence of a narrow Ca-DOS peak at the conduction band edge.[34] These Ca states are however weakly coupled with the electronic structure of the host system (p-Sb and d-Co states), since at moderately low Ca concentration ($y=0.05$) the Fermi level was confined in a sharp narrow peak of s-Ca states. This peak tends to broaden when the Ca content increases, mainly due to strengthened hybridization between s-Ca and d-Co states. It was concluded that the appearance of the s-like narrow peak from inserted Ca at the bottom of the conduction band edge was responsible for the particular electronic

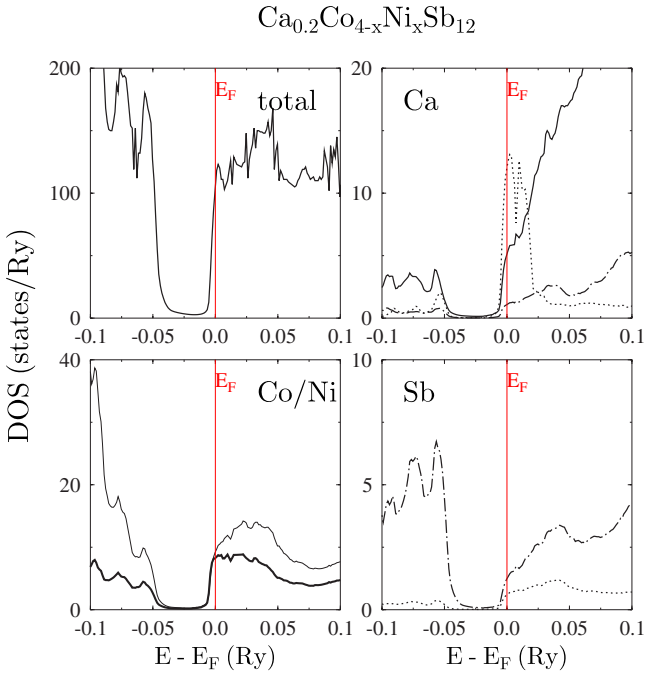

FIG. 9. (Color online) KKR-CPA density of states in $Ca_{0.20}Co_{4-x}Ni_xSb_{12}$ (x=0.04). Total and l-decomposed DOS (s—dotted, p—dot-dashed, d—full lines) of constituent atoms are shown. In the case of Co (thin line) and Ni (thick line), s and p contributions are not plotted for sake of clarity. E_F=0 is marked by a vertical red line.

transport behavior of these systems, as revealed from electronic transport, specific heat and magnetic susceptibility measurements.[34]

Figures 8 and 9 present the total and l-decomposed DOS in $Ca_{0.10}Co_{3.96}Ni_{0.04}Sb_{12}$ and $Ca_{0.20}Co_{3.96}Ni_{0.04}Sb_{12}$, respectively. At a first glance, we see that the Fermi level (put always at zero) is located just above the energy gap, in strongly increasing DOS. Although these states are attributed mainly to d states of Co and p states of Sb, the largest atomic contribution to $N_{tot}(E_F)$, comes from s-Ca states. This electronic structure behavior should have an important effect on the electron transport properties of $Ca_yCo_{4-x}Ni_xSb_{12}$, especially at low temperatures. It is interesting to note that in spite of marked modifications of the electronic states near the conduction band edge with y content,[34] conversely, the replacement of Co by Ni does not change noticeably the electronic structure near E_F. These variations can be well interpreted within the rigid band model (Co and Ni d-DOS in Figs. 8 and 9). Such behavior is expected from rather similar crystal potentials of Ni impurity (on Co site) and Co atoms in the skutterudite systems. The d-DOS near the conduction band states are very close for both transition elements, especially concerning the DOS slopes above the energy gap. Noteworthy, this is not the case when observing Co and Ni valence states located below the energy gap. Alloying with Ni only slightly increases the DOS value of $N_{tot}(E_F)$ due to the Fermi level shift into the conduction bands and finally the Co contribution to DOS at E_F in $Ca_yCo_{4-x}Ni_xSb_{12}$ becomes more important than in the corresponding Ni-free $Ca_yCo_4Sb_{12}$ samples.[34] On the whole, the DOS at E_F calculated for some illustrative compositions (Table II) show that variation of both Ca content and different levels of substitution on Co site by Ni, make the electronic structure in the vicinity of the Fermi level very sensitive to the alloying level (also seen from comparison of y=0.10 and y=0.20 in Figs. 8 and 9). The numerical values change rather irregularly when both Ca and Ni contents vary. Such complex behavior are likely due to the fact that at defined Ca content, Ni-alloying scans to some extent a sharp peak of s-Ca states (this peak additionally changes its shape when y varies). The contributions of the d states of the transition metals also slightly change when the Ni content increases. Consequently, electronic interactions in the vicinity of E_F (overlapping of s-Ca and d states of Co/Ni and also p-Sb states) depend on x and y in not a simple way. This locally modifies the total DOS at E_F but also its slope. Both these electronic structure characteristics may result in fluctuations of the calculated thermopower with Ni concentration (see below). The simple trends revealed for Ni-free $Ca_yCo_4Sb_{12}$ samples,[34] i.e., the Seebeck coefficient decreases with y, are less evident to detect when additionally nickel is alloyed.

In order to have more quantitative insight into the observed behavior of thermopower of $Ca_yCo_{4-x}Ni_xSb_{12}$ as a function of Ni-alloying and Ca content, the Seebeck coefficient slopes, S/T, have been estimated from the numerical derivative of total DOS in the vicinity of the Fermi level, using the simplified Mott's formula

$$\frac{S}{T} = -\pi^2 k_B^2/3e \left.\frac{d\ln\sigma(E)}{dE}\right|_{E=E_F} \approx -\left.\frac{1}{N_{tot}(E)}\frac{dN_{tot}(E)}{dE}\right|_{E=E_F} \quad (1)$$

where $\sigma(E)$ denotes the electrical conductivity, and k_B the Boltzmann constant.

TABLE II. Total DOS (in states/Ry/spin per formula unit) and site-decomposed DOS (in states/Ry/spin per atom) calculated at the Fermi level in $Ca_yCo_{4-x}Ni_xSb_{12}$ for different concentrations of Ca (y=0.10 and 0.20) and Ni (x=0, 0.04 and 0.08) from KKR-CPA calculations.

	$Ca_{0.10}Co_{4-x}Ni_xSb_{12}$				$Ca_{0.20}Co_{4-x}Ni_xSb_{12}$			
x	N_{tot}	n_{Ca}	n_{Co}	n_{Ni}	N_{tot}	n_{Ca}	n_{Co}	n_{Ni}
0.0	34.3	10.2	3.7	3.6	49.4	9.3	4.7	4.2
0.04	43.3	9.8	3.8	3.7	54.9	9.1	4.7	4.1
0.08	45.6	9.5	4.3	4.0	56.0	9.0	4.8	4.1

TABLE III. Illustrative thermopower S_{cal} (in μV/K) as estimated from KKR-CPA DOS derivative at the Fermi level in $Ca_{0.10}Co_{4-x}Ni_xSb_{12}$ and $Ca_{0.20}Co_{4-x}Ni_xSb_{12}$ at 40 and 80 K (see the text). The values are compared to the experimental values (S_{exp}) given if possible for the closest composition available.

	$Ca_{0.10}Co_{4-x}Ni_xSb_{12}$				$Ca_{0.20}Co_{4-x}Ni_xSb_{12}$			
x	T=40 K		T=80 K		T=40 K		T=80 K	
	S_{cal}	S_{exp}	S_{cal}	S_{exp}	S_{cal}	S_{exp}	S_{cal}	S_{exp}
0.0	−28	−27	−55	−50	−17	−23	−34	−35
0.04	−30	−50	−60	−80	−15	−35	−30	−59
0.08	−16		−32		−13		−26	

If $N_{tot}(E)$ is the total density of states given in states Ry^{-1}, the S/T ratio in currently used units of thermopower can be obtained from the relation S/T ($\mu V/K^2$)$=0.2877\times10^{-2}$ $d \ln N_{tot}(E)/dE$. It should be noted that in this approach one neglects the energy dependence of the carrier mobility $\mu(E)=\mu_0$, namely $\sigma(E)\propto N_{tot}(E)\mu_0$, but it allows an approximate analysis of Seebeck coefficient. The calculated values of S [from Eq. (1)] are presented in Table III for two Ca contents (y=0.10 and 0.20) and different Ni concentrations at two arbitrary chosen low temperatures (40 K and 80 K), together with experimental values of close composition when available. It illustrates that the values obtained for the y =0.10 series of compounds increases at small Ni contents (x=0.04) and then decreases when the Ni content increases (x=0.08). This tentatively supports experimental findings, but the obtained theoretical values are smaller that the experimental ones. For higher Ca content (y=0.20 series of compounds), the KKR-CPA calculations predict that the Seebeck coefficient should monotonically decrease when alloying with Ni contents increases, which is not observed experimentally, since in this series of compounds the measured Seebeck coefficient (at low temperature) markedly increases with Ni doping. On the whole, one observes rather good agreement between theoretical and experimental points for Ni-free samples, whereas the agreement in not satisfying for Ni-substituted $Ca_yCo_{4-x}Ni_xSb_{12}$ skutterudites, since the theoretical values are smaller than the experimental ones.

The calculation of low temperature thermopower, based uniquely on the DOS analysis, seems to underestimate the measured values and can only be used as a qualitative explanation of large S values in the investigated samples. More accurate calculations accounting for kinetic parameters of carriers are necessary to better explain the low temperature electron transport properties in Ni-substituted $Ca_yCo_{4-x}Ni_xSb_{12}$ skutterudites (see Sec. III C). On the other hand, the direct comparison between experimental and theoretical values is not easy due to not similar contents of Ca and Ni in the two investigated series of compounds.

C. Origin of low electrical resistivity values and high thermopower absolute values

The KKR-CPA calculations showed that the addition of Ni in $Ca_yCo_4Sb_{12}$ leads to a slight increase of the density of states at E_F (due to the shift of the Fermi level into the conduction states in more or less a rigid way). Furthermore, the presence of d-Ni states at the Fermi level (just above the gap) suggests that in the Ni-containing samples, the electrical conductivity is related not only to heavy electrons attributed to Ca insertion (a strong peak at the conduction band edge, Figs 8 and 9) but also to more mobile electrons with lighter effective masses (seen from less sharp variation of the Co/Ni-DOS, Figs 8 and 9). These electronic structure features suggest the existence of two mechanisms responsible for the low temperature electrical conductivity behavior in $Ca_yCo_{4-x}Ni_xSb_{12}$ systems, which seem not to be the case in $Ca_yCo_4Sb_{12}$ skutterudites.

We have also seen that minute alloying with Ni does not noticeably modify the total DOS shape near the Fermi level due to the aforementioned rigid-like behavior (Ni- and Co-DOS in Figs 8 and 9). This may tentatively explain why the high thermopower values measured in the Ca-partially filled skutterudites are preserved when Ni is added. Our conclusion is in line with the large S/T slope obtained from numerical derivation of the DOS curves at E_F. The linear term seems to dominate at low temperature, as detected from the experimental thermopower behaviors $S(T)$ in Fig. 5.

We have shown experimentally that the decrease of the electrical resistivity in the Ni-containing samples and the conservation of the high thermopower values are responsible for the enhanced thermoelectric performance. Two factors contribute to the decrease of the electrical resistivity: an increase of the number of carriers (at least for the series $y\sim0.18$) and an increase of the carrier mobility (μ) as suggested from the Hall experiments. The analysis of the imaginary part of the KKR-CPA complex energy bands $E(k)$ and the resulting electron lifetime [τ=Im $E(k)/h$, h—Planck constant], related to the effect of chemical disorder,[41] sheds a light on charge mobility behavior observed in Ni-doped samples. In the particular case of $Ca_{0.2}Co_{4-x}Ni_xSb_{12}$ (x=0.0, 0.04 and 0.08), we did not notice however marked variations of the τ value near the Fermi surface with increasing Ni content. This was verified for three important directions (P-Γ-H-N) (Fig. 10), where the bands cross E_F. Thus, in view of these results, the abrupt increase of carrier mobility μ observed in Ni-doped samples (Table II) should be rather attributed, according to the well-known relation $\mu\sim\tau/m_{eff}$, to an occurrence of much smaller effective masses (m_{eff}) of electrons with respect to those in Ni-free systems. This picture is partly supported by the presence of a very flat band "wrapped" around E_F along the Γ-H direction as derived from the real part of the complex dispersion curves (Fig. 10).

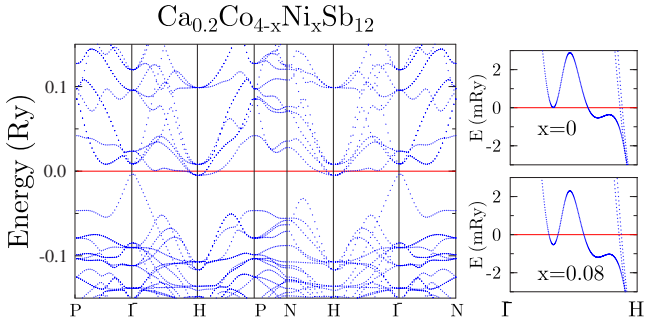

FIG. 10. (Color online) Left panel: Real part of complex energy bands $E(k)$ in $Ca_{0.10}Co_{4-x}Ni_xSb_{12}$ ($x=0.01$) as derived from KKR-CPA calculations. $E_F=0$. For sake of clarity, dispersion curves near the Fermi level are only plotted. Right panel: A flat band along the Γ-H direction with enlarged energy scale (mRy) and an appearance of electron-like Fermi surface pocket with Ni-doping ($x=0$ and 0.08).

With Ni-doping, an additional electronlike pocket tends to open, which is well seen on enlarged plot with highly dense k-point grid (right panel in Fig. 10). The band crossing E_F (Γ-H) exhibits more important energy dispersion that would indicate lighter effective masses than in the $x=0$ case. Except for the aforementioned Fermi surface modification, electronic bands near E_F remain practically unchanged upon Ni doping, and as encountered in $Ca_yCo_4Sb_{12}$,[34] high electron effective masses are still preserved in $Ca_yCo_{4-x}Ni_xSb_{12}$.

More quantitative answer from band theory, as far as the electrical conductivity and thermopower behavior are concerned, could be expected after precise numerical investigations of electron velocity and electron life-time at the Fermi surface (as recently performed for half-Heusler systems).[41] However, the self-consistent computations of electron transport coefficients are highly time-consuming and complex for the disordered $Ca_yCo_{4-x}Ni_xSb_{12}$ skutterudites, if accounting for chemical disorder on two crystallographic sites.

IV. SUMMARY AND CONCLUSIONS

As the thermoelectric properties of n type $Ca_yCo_4Sb_{12}$ skutterudites remained quite modest at high temperatures with regard to performance, improvement was attempted by Ni alloying. This operation proved to be very efficient for decreasing the electrical resistivity while keeping low the values of the thermal conductivity and high the values of the thermoelectric power. These behaviors can be attributed to a change of the conductivity mechanisms of the charge carriers as suggested from the analysis of the electronic density of states.

The negative and important values of the Seebeck coefficient as well as the substantial decrease of the electrical resistivity when substituting Co by Ni in $Ca_yCo_{4-x}Ni_xSb_{12}$ skutterudites can be qualitatively well interpreted in view of electronic structure features near the Fermi level as derived from KKR-CPA calculations.

ACKNOWLEDGMENTS

The authors would like to thank M. Dehmas for his help in the thermal diffusivity measurements. The authors acknowledge support from ADEME and the European Network of Excellence CMA "Complex Metallic Alloys."

*Corresponding author. Email address: lenoir@mines.inpl-nancy.fr

[1] *Thermoelectrics Handbook, Macro to Nano*, edited by D. M. Rowe (CRC Press, Taylor & Francis Group, Boca Raton FL, 2006).
[2] C. Uher, in *Semiconductors and Semimetals*, edited by T. Tritt (Academic, San Diego, 2000), Vol. 69, p. 139.
[3] A. Dauscher, B. Lenoir, H. Scherrer, and T. Caillat, in *Recent Research Developments in Materials Science*, edited by S. G. Pandalai (Research Signpost, 2002), Vol. 3, p. 181.
[4] D. T. Morelli, G. P. Meisner, B. Chen, S. Hu, and C. Uher, Phys. Rev. B **56**, 7376 (1997).
[5] G. S. Nolas, J. L. Cohn, and G. A. Slack, Phys. Rev. B **58**, 164 (1998).
[6] N. R. Dilley, E. D. Bauer, M. B. Maple, and B. C. Sales, J. Appl. Phys. **88**, 1948 (2000).
[7] G. S. Nolas, M. Kaeser, R. T. Littleton IV, and T. M. Tritt, Appl. Phys. Lett. **77**, 1855 (2000).
[8] B. C. Sales, B. C. Chakoumakos, and D. Mandrus, Phys. Rev. B **61**, 2475 (2000).
[9] G. S. Nolas, H. Takizawa, T. Endo, H. Sellinschegg, and D. C. Johnson, Appl. Phys. Lett. **77**, 52 (2000).
[10] L. D. Chen, T. Kawahara, X. F. Tang, T. Goto, T. Hirai, J. S. Dyck, W. Chen, and C. Uher, J. Appl. Phys. **90**, 1864 (2001).
[11] G. A. Lamberton Jr., S. Bhattacharya, R. T. Littleton IV, M. A. Kaeser, R. H. Tedstrom, T. M. Tritt, J. Yang, and G. S. Nolas, Appl. Phys. Lett. **80**, 598 (2002).
[12] V. L. Kuznetsov, L. A. Kuznetsova, and D. M. Rowe, J. Phys.: Condens. Matter **15**, 5035 (2003).
[13] G. S. Nolas, J. Yang, and H. Takizawa, Appl. Phys. Lett. **84**, 5210 (2004).
[14] M. Puyet, B. Lenoir, A. Dauscher, M. Dehmas, C. Stiewe, and E. Müller, J. Appl. Phys. **95**, 4852 (2004).
[15] X. Y. Zhao, X. Shi, L. D. Chen, W. Q. Zhang, W. B. Zhang, and Y. Z. Pei, J. Appl. Phys. **99**, 053711 (2006).
[16] T. He, J. Chen, H. D. Rosenfeld, and M. A. Subramanian, Chem. Mater. **18**, 759 (2006).
[17] M. Puyet, B. Lenoir, A. Dauscher, P. Weisbecker, and S. J. Clarke, J. Solid State Chem. **177**, 2138 (2004).
[18] C. Uher, in *Proceedings of the 21th International Conference on Thermoelectrics* (IEEE, New York, 2002), p. 35.
[19] L. D. Dudkin and N. Kh. Abrikosov, Zh. Neorg. Khim. **2**, 212 (2002).
[20] T. Caillat, A. Borshchevsky, and J.-P. Fleurial, J. Appl. Phys. **80**, 4442 (1996).
[21] H. Anno, K. Matsubara, Y. Notohora, T. Sakakibara, and H. Tashiro, J. Appl. Phys. **86**, 3780 (1999).
[22] J. S. Dyck, W. Chen, J. Yang, G. P. Meisner, and C. Uher, Phys. Rev. B **65**, 115204 (2002).

[23] H. Kitagawa, M. Wakatsuki, H. Nagaoka, H. Noguchi, Y. Isoda, K. Hasezaki, and Y. Noda, J. Phys. Chem. Solids **66**, 1635 (2005).
[24] Y. Nagamoto, K. Tanaka, and T. Koyanagi, in *Proceedings of the 17th International Conference on Thermoelectrics* (IEEE, New York, 1998), p. 302.
[25] K. T. Wojciechowski, J. Tobola, and J. Leszczynski, J. Alloys Compd. **361**, 19–27 (2003).
[26] X. Y. Li, L. D. Chen, J. F. Fan, W. B. Zhang, T. Kawahara, and T. Hirai, J. Appl. Phys. **98**, 083702 (2005).
[27] J. S. Dyck, W. Chen, C. Uher, L. Chen, X. Tang, and T. Hirai, J. Appl. Phys. **91**, 3698 (2002).
[28] M. Puyet, B. Lenoir, A. Dauscher, M. Dehmas, C. Stiewe, E. Müller, and J. Hejtmanek, J. Appl. Phys. **97**, 083712 (2005).
[29] X. Li, X. Zhao, S. Bai, Y. Pei, and L. Chen, in *Proceeding of the 25th International Conference on Thermoelectrics* (IEEE, New-York, 2006).
[30] L. Rauscher, E. Müller, H. T. Kaibe, H. Ernst, and W. A. Kaysser, in *Proceeding of the 19th International Conference on Thermoelectrics*, ed. Rowe D. M. (Babrow Press, UK, 2000), p. 395.
[31] A. Bansil, S. Kaprzyk, P. E. Mijnarends, and J. Tobola, Phys. Rev. B **60**, 13396 (1999).
[32] S. Kaprzyk and A. Bansil, Phys. Rev. B **42**, 7358 (1990).
[33] T. Stopa, S. Kaprzyk, and J. Tobola, J. Phys.: Condens. Matter **16**, 4921 (2004).
[34] M. Puyet, B. Lenoir, A. Dauscher, P. Pécheur, C. Bellouard, J. Tobola, and J. Hejtmanek, Phys. Rev. B **73**, 035126 (2006).
[35] M. Puyet, C. Candolfi, L. Chaput, V. Da Ros, A. Dauscher, B. Lenoir, and J. Hejtmanek, J. Phys.: Condens. Matter **18**, 11301 (2006).
[36] D. J. Singh and W. E. Pickett, Phys. Rev. B **50**, 11235 (1994).
[37] J. O. Sofo and G. D. Mahan, Phys. Rev. B **58**, 15620 (1998).
[38] I. Lefebvre-Devos, M. Lassalle, X. Wallart, J. Olivier-Fourcade, L. Monconduit, and J. C. Jumas, Phys. Rev. B **63**, 125110 (2001).
[39] K. Koga, K. Akai, K. Oshiro, and M. Matsuura, Phys. Rev. B **71**, 155119 (2005).
[40] L. Chaput, P. Pecheur, J. Tobola, and H. Scherrer, Phys. Rev. B **72**, 085126 (2005).
[41] T. Stopa, J. Tobola, S. Kaprzyk, E. K. Hlil, and D. Fruchart, J. Phys.: Condens. Matter **18**, 6379 (2006).